HHS Public Access

Author manuscript

Exp Neurol. Author manuscript; available in PMC 2018 November 01.

Published in final edited form as:

Exp Neurol. 2017 November ; 297: 82–91. doi:10.1016/j.expneurol.2017.07.016.

Endotoxemia induces lung-brain coupling and multi-organ injury following cerebral ischemia-reperfusion

Nguyen Mai, Ph.D.[1], **Landa Prifti, B.S.**[1], **Aric Rininger, B.S.**[1], **Hannah Bazarian, B.S.**[1], and **Marc W. Halterman, M.D., Ph.D.**[1,2]

[1]Center for Neurotherapeutics Discovery, University of Rochester, Rochester, NY 14642

[2]Department of Neurology, University of Rochester, Rochester, NY 14642

Abstract

Post-ischemic neurodegeneration remains the principal cause of mortality following cardiac resuscitation. Recent studies have implicated gastrointestinal ischemia in the sepsis-like response associated with the post-cardiac arrest syndrome (PCAS). However, the extent to which the resulting low-grade endotoxemia present in up to 86% of resuscitated patients affects cerebral ischemia-reperfusion injury has not been investigated. Here we report that a single injection of low-dose lipopolysaccharide (50 μg/kg, IP) delivered after global cerebral ischemia (GCI) induces blood-brain barrier permeability, microglial activation, cortical injury, and functional decline *in vivo*, compared to ischemia alone. And while GCI was sufficient to induce neutrophil (PMN) activation and recruitment to the post-ischemic CNS, minimal endotoxemia exhibited synergistic effects on markers of systemic inflammation including PMN priming, lung damage, and PMN burden within the lung and other non-ischemic organs including the kidney and liver. Our findings predict that acute interventions geared towards blocking the effects of serologically occult endotoxemia in survivors of cardiac arrest will limit delayed neurodegeneration, multi-organ dysfunction and potentially other features of PCAS. This work also introduces lung-brain coupling as a novel therapeutic target with broad effects on innate immune priming and post-ischemic neurodegeneration following cardiac arrest and related cerebrovascular conditions.

Keywords

global cerebral ischemia; post-cardiac arrest syndrome; endotoxin; systemic inflammation; ischemia-reperfusion injury; neurodegeneration; neuroinflammation; microglia; neutrophil; blood-brain barrier

Corresponding Author: Marc W. Halterman, M.D., Ph.D., Department of Neurology, Center for Neurotherapeutics Discovery, University of Rochester Medical Center, 601 Elmwood Avenue, Box 645, Rochester, NY 14642, (585) 273-1335, marc_halterman@urmc.rochester.edu.

CONFLICTS OF INTEREST/DISCLOSURES

None.

1. INTRODUCTION

An estimated 500,000 patients suffer cardiac arrest in the United States annually, and despite the introduction of induced hypothermia, the prognosis for meaningful neurological recovery remains poor in over 80% of cases (Bernard, et al. 2002, Hoesch, et al. 2008). These dire clinical outcomes reflect the exquisite vulnerability of the central nervous system (CNS) to acute ischemic challenge as well as the delayed effects of reperfusion in the context of systemic injury. Collectively referred to as the post-cardiac arrest syndrome (PCAS), this disorder is characterized by changes in hemostasis and microvascular rheology, adrenal insufficiency with resulting shock physiology, heightened levels of inflammation, and delayed damage to both the CNS and peripheral organs (Adrie, et al. 2004, Neumar, et al. 2008).

The link between systemic inflammation and poor outcomes in patients presenting with this and other forms of acute neurological injury is well recognized (Becker, et al. 2011, Kliper, et al. 2013, Rodriguez, et al. 2013). In the case of cardiac arrest, tissue ischemia stimulates the activity of transcription factors including hypoxia-inducible factor-1α and nuclear factor-κB that stimulate the production of pro-inflammatory cytokines and enhance other aspects of host immune function (Paradis 2007, Ridder and Schwaninger 2009). Ischemic damage also induces a sterile inflammatory response through the release of damage-associated molecular patterns (DAMPs) from the brain and other tissues (Pittman and Kubes 2013, Tadie, et al. 2013, Wang, et al. 2015). More recently, studies have revealed detectable levels of endotoxin in the serum of up to 86% of patients within 24–48 hours following return of spontaneous circulation (Adrie, et al. 2002, Grimaldi, et al. 2013, Grimaldi, et al. 2015, L'Her, et al. 2005). The presence of endotoxin and other pathogen-associated molecular patterns (PAMPs) has been linked with ischemia-induced growth of gram-negative intestinal flora and loss of mucosal barrier function with secondary bacteremia (Adrie, et al. 2002, Karhausen, et al. 2013, Wang, et al. 2012). While endotoxemia has been associated with durable neurocognitive deficits in patients surviving *Escherichia coli* sepsis (Annane and Sharshar 2015), the levels of lipopolysaccharide (LPS) detected in cases of sepsis are typically higher than those reported following cardiac arrest (2.6 *vs.* <0.6 EU/ml) (Casey, et al. 1993, Grimaldi, et al. 2015). And while linked to increased risk of shock and organ failure (Grimaldi, et al. 2013), the effects and consequences of serologically undetectable endotoxemia on cerebral ischemia-reperfusion injury remain unexplored.

The pathological changes in the brain caused by global cerebral ischemia (GCI) have been widely studied and involve both the cell-autonomous and non-cell-autonomous effects of cardiac arrest (Blomqvist and Wieloch 1985, Hossmann and Hossmann 1973). Models of GCI are often used to model delayed neurodegeneration within the CA1 field of the hippocampus; however, additional regions of the brain including the thalamus, basal ganglia, and cortex may also be affected (Deierborg, et al. 2008, Thal, et al. 2010). And while selective neuron vulnerability is the sine qua non of GCI, associated post-ischemic changes include microgliosis, and damage to the cerebrovasculature characterized by endothelial dysfunction, and loss of blood-brain barrier (BBB) integrity (Yao, et al. 2015). Preclinical models of GCI typically involve the isolation of the cerebral and systemic circulation via occlusion of 2 or more extracranial vessels (Ito, et al. 2013, Pulsinelli and Brierley 1979,

Thal, et al. 2010, Yonekura, et al. 2004). While intrinsic CNS mechanisms leading to neuronal loss remain an important therapeutic target (Coultrap, et al. 2011), GCI models do not recapitulate multi-organ injury and other features of PCAS. Thus, making headway in identifying therapies to disrupt post-arrest neurological decline will require a better understanding of the complex interplay between the brain's intrinsic response to ischemia and the extrinsic changes in the periphery involving cellular immunity as well as the production of other factors with long-range signaling properties.

To better understand the mechanism(s) underlying catastrophic brain injury in PCAS, we studied the effect of low-dose endotoxin challenge on brain injury in a mouse model of GCI. Our results indicate that serologically undetectable endotoxemia increased levels of cortical injury, microglial activation, microvascular injury, and behavioral compromise beyond what is observed after ischemic injury alone. We also observed marked neutrophil (PMN) activation, lung injury, and the accumulation of PMNs in the brain, lung, and other non-ischemic tissues with combined challenge. Our data suggest that therapies geared towards blocking the effects of systemic endotoxin in patients surviving cardiac arrest may be an effective strategy to limit multi-organ dysfunction commonly observed in the post-resuscitation period. Furthermore, these results implicate lung-brain coupling as an important determinant of post-ischemic neurodegeneration mediated through effects on innate immunity.

2. MATERIALS AND METHODS

2.1 Endotoxin Titration

All mouse work was performed according to federal regulations with approval by the University Committee on Animal Resources. C57BL/6 mice (5-8-week-old males, 25–30 g, n = 3) received intraperitoneal (IP) injections of either saline (SAL) or LPS (50 μg/kg, 4 mg/kg, or 20 mg/kg; derived from *E. coli* O111:B4; Sigma-Aldrich, St. Louis, MO) to mimic endotoxin leak during gut injury. LPS doses were tested to determine which yielded serum endotoxin levels comparable to those observed in patients admitted after cardiac arrest (Adrie, et al. 2002, Grimaldi, et al. 2013). Retro-orbital blood was collected at baseline, 6, 24, 48, and 72 hours after injection for granulocyte counts using a Vetscan HM5 blood analyzer (Abaxis, Union City, CA), and endotoxin measurement using the limulus amebocyte lysate assay as used by Adrie et. al. in their clinical studies (Thermo Fisher, Waltham, MA) (Adrie, et al. 2002). Serum samples were diluted 50-fold to minimize hemoglobin contamination for the chromogenic assay. Assessment of plasma IL-6, IL-1β, and TNF-α was performed using the LEGENDplex immunoassay (Biolegend, San Diego, CA). Weight and rectal temperature were recorded at each time point (Figure S1).

2.2 Global Cerebral Ischemia Model

Male C57BL/6 mice were randomized into Sham/SAL, Sham/LPS, 3VO/SAL, and 3VO/LPS groups (Figure 2A). On Day −10, all mice underwent basilar artery occlusion (BAO) as described (Thal, et al. 2010). After recovery (Day 0), the 3VO group underwent 15 minutes of bilateral common carotid artery occlusion (BCCAO) with controls undergoing neck dissection without occlusion. Mice were excluded if cerebral blood flow (CBF) by

Laser Doppler flowmetry (Perimed, Ardmore, PA) did not fall below 70% during 3VO (Figure S2). Within 1 minute of reperfusion, groups received either a single IP injection of 50 μg/kg LPS or saline. Daily weights and rectal temperatures were recorded (Figure 2B–C). Day 3 group sizes after Doppler exclusion were as follows: Sham/SAL (n = 4), Sham/LPS (n = 4), 3VO/SAL (n = 4), and 3VO/LPS (n = 3). In preliminary studies, we found that cerebral injury caused by 3VO/SAL was 24.31 ± 4.39%, and injury caused by 3VO/LPS was 39.95 ± 10.87%. Sample sizes for this study ($n \geq 2$) were calculated using these means with σ as the standard deviation of the 3VO/SAL group. For this analysis, $\alpha = 0.05$, power = 0.9, and sampling ratio = 1.

2.3 Behavioral Analyses

Global neurological function was assessed using a composite scoring system adapted from Abella et al. (Table S1) (Abella, et al. 2004). Domains tested included assessments of level of consciousness, spontaneous movement, gait, touch escape response, corneal reflex, and respiration. Scores for each domain ranged from 0–2, with 2 indicating normal function; maximal score for this assay was 12. Neurological assessments were performed on Days −10 prior to BAO, 0 prior to BCCAO or sham, 1, and 3 by an investigator blinded to the intervention.

2.4 Immunohistochemical and Image Analyses

Tissues were removed following intracardiac perfusion, post-fixed in 4% paraformaldehyde (Sigma-Aldrich), cut into 25 μm sections, and stored at 4°C in cryoprotectant. Sections were washed with PBS and blocked in 10% goat serum for 1 hour at 20°C prior to immunohistochemical (IHC) staining (see Supplemental Methods & Table S2). Fluoro-Jade C staining of brain sections was performed as described (Schmued, et al. 2005). Sections were imaged using an OptiGrid Structured-Light Imaging System (Qioptiq, Fairport, NY). Cortical Ly-6B(+) neutrophil (PMN) counts and percent injury calculations based on regional loss of MAP2 staining were calculated from images taken from 5 matched, non-contiguous coronal sections spanning +1.32 and −2.92 mm from bregma. Percent injury based on MAP2 staining was calculated from thresholded images as the area of MAP2(−) tissue divided by total cortical surface area. Platelet endothelial cell adhesion molecule-1 (PECAM-1) upregulation and IgG deposition were measured by the mean gray value (fluorescence intensity) from random sections imaged at 10x magnification per animal. Fluorescence intensities were normalized to PECAM-1(+) vessel length (cm). Microglial activation was measured by the mean gray value of Iba1 from random sections imaged at 10x magnification per animal. Sholl analyses were conducted with ≥10 microglia per animal imaged at 63x magnification (Ferreira, et al. 2014). PMN infiltration was estimated in lung (due to high PMN density) by measurement of Ly-6B mean gray value, and counts were obtained from random sections of liver and kidney; images for these quantifications were acquired at 40x magnification. Alveolar wall thickness was measured as the smallest orthogonal distance between 2 adjacent alveoli. Images were acquired using identical settings and values and analyzed using ImageJ (http://rsb.info.nih.gov/ij/). Liver and kidney sections were also stained with hematoxylin and eosin to evaluate for tissue injury (Cardiff, et al. 2014).

2.5 Flow Cytometry

For flow cytometric analyses of endotoxin experiments, blood, lungs, and spleens were collected 6 hours after 50 μg/kg LPS injection. Organs were dissociated by agitation in RPMI with 1 mg/ml collagenase II for 30 minutes. For 3VO experiments, flow cytometric analyses were performed on retro-orbital blood collected at 2 hours, 4 hours, and 6 hours after experimental surgery. Whole blood was washed and lysed with red cell lysis buffer (Biolegend, San Diego, CA) for 5 minutes at 4°C. Cells were stained with FITC-labeled anti-Ly-6G (1 μg/ml; 30 minutes, 4°C) and Alexa Fluor 647-labeled anti-CD11b antibodies (0.8 μg/ml) with 4 μl Fc receptor block per sample. Cells were later fixed in 2% paraformaldehyde for 30 minutes (Highland, et al. 2016), and fluorescence was measured using a BD FACSCanto II Flow Cytometer (BD Biosciences, San Jose, CA). Data were collected for 10,000 events, and the following gating strategy was used: a forward *vs.* side scatter plot (FSC-area *vs.* SSC-area) was used to visually identify white blood cells and exclude debris. Gates were then manually drawn on plots of FSC-height *vs.* FSC-area plots to remove cell doublets. Two-dimensional plots of Ly-6G *vs.* CD11b were used to identity Ly-6G^{hi}/CD11b^{hi} PMNs, and histograms were constructed for each PMN population. Geometric mean fluorescence intensity (MFI) analyses were performed using FlowJo analysis software (TreeStar, Ashland, OR).

2.6 Statistical Analyses

Statistical analyses were performed using Prism (Graphpad, La Jolla, CA) and MATLAB (Mathworks, Natick, MA). Data are expressed as averages with standard deviations. In the LPS dosing experiment, changes in plasma endotoxin, cytokines, granulocyte count, weight, and temperature were analyzed by repeated measures analysis of variance (ANOVA) with Holm-Sidak post hoc test. In experiments involving Sham/3VO and SAL/LPS, comparisons were made using 2-way ANOVA and Holm-Sidak post hoc test for cortical injury, PECAM-1 upregulation, IgG deposition, Iba1 upregulation, and PMN infiltration. Differences in microglial arborization were calculated using repeated measures ANOVA for the number of intersections at each radius from the soma. Changes in weight, core temperature, and neurological function over time were analyzed using 3-way ANOVA and Dunn-Sidak post hoc test. Relationships between PMN infiltration and cortical injury, PMN infiltration and Neurological Function Score, and CBF and cortical injury were determined with Pearson's correlation coefficient. *P* values less than 0.05 were considered significant.

3. RESULTS

3.1 Physiological and behavioral effects of 3VO/LPS treatment

Our initial goal was to determine which LPS dose(s) would recapitulate levels of endotoxemia observed clinically. Intraperitoneal administration of 4 mg/kg LPS produced peak serum endotoxin levels (0.95 ± 0.14 EU) within 6 hours (Figure 1A). After correcting for sample dilution, this was comparable to levels seen in patients within the first 24–72 hours following cardiac arrest (Adrie, et al. 2002, Grimaldi, et al. 2013). However, treatment with doses as low as 1 mg/kg LPS resulted in significant mortality when combined with global ischemia precluding their use (data not shown). Standard LPS dosing of between 4–20 mg/kg also exerted variable effects on granulocyte counts, core temperature and post-

procedure weights (Figure 1B–D). Given the potential confounding effects on downstream analyses, we tested the effects of low-dose LPS (50 μg/kg), which produced no discernable effect on serum endotoxin levels, granulocyte counts, core temperature, or weight. Also, in contrast to 20 mg/kg LPS, low-dose treatment produced only a transient increase in serum IL-6, which was not higher than levels observed in saline-treated controls (Figure 1E). No changes were observed with IL-1β or TNF-α. After establishing the effects of higher LPS doses, we sought to determine whether 50 μg/kg LPS, while serologically undetectable, still had effects on PMN activation. Six hours after IP injection, 50 μg/kg LPS increased MFI of the activation marker CD11b on PMNs in peripheral blood (7,234 *vs.* 2,012) and on PMNs marginated in the lung (26,588 *vs.* 14,486) and spleen (30,781 *vs.* 15,630) compared to saline injection.

To study the effects of low-dose endotoxin on the post-ischemic neurodegeneration, mice received either saline or IP LPS injection after completion of either sham or the 3VO procedure (Figure 2A). Laser Doppler flowmetry was used to confirm adequate reductions in cerebral blood flow in mice treated with ischemia alone (3VO/SAL) or ischemia combined with systemic LPS (3VO/LPS; Figure S2). Three-way ANOVA revealed effects of inflammation ($p = 0.0378$), ischemia ($p = 0.0013$), and time after experimental manipulation ($p = 0.0005$) on weight, and effects of ischemia ($p < 0.0001$) and time ($p < 0.0001$) on core temperature (Figure 2B–C). While LPS treatment alone induced fever (Day 0–3, $p = 0.0146$), mice in the 3VO/LPS cohort exhibited a non-significant trend towards hypothermia between Day 2 and 3 ($p = 0.0826$) as previously reported (Peres Bota, et al. 2004). Mice undergoing 3VO/SAL exhibited a decline in global neurological function using a composite battery of tests administered 3 days following reperfusion (9.38 ± 2.25) compared to Sham/SAL (12.00 ± 0.00; $p = 0.0015$), and deficits were worse in mice undergoing 3VO/LPS (4.00 ± 1.80; $p = 0.0016$ *vs.* 3VO/SAL) (Figure 2D).

3.2 Histological assessment of cortical injury and neuroinflammation

We next assessed the temporal and spatial aspects of neuronal injury by performing IHC in each of the 4 treatment groups (Figure 3). After 3 days of reperfusion, distinct regions of cortical injury characterized by the loss of neuron-specific microtubule-associated protein 2 (MAP2) and the accumulation of Fluoro-Jade C(+) neurons were observed (Figure 3A, top) (Chamak, et al. 1987, Popp, et al. 2009, Schmued, et al. 2005). While we observed axonal beading and Fluoro-Jade C staining within the CA1 region of the hippocampus (Figure 3A, bottom), hippocampal injury was less severe and more inconsistent compared to that observed in the cortical hemispheres. Occlusion of the basilar artery conducted during the first stage of the 3VO procedure caused minimal cortical injury in the sham surgical controls (Sham/SAL, 7.87 ± 1.76%; Sham/LPS, 11.89 ± 0.99%). By Day 3, mice exposed to combined 3VO/LPS treatment (39.79 ± 7.28%) were more severely affected than those treated with only global ischemia (3VO/SAL, 25.82 ± 4.61%; $p = 0.047$) (Figure 3B).

In addition to exerting potent effects on immune cells, endotoxin causes local inflammation and damage to the vasculature when combined with 3VO (Denes, et al. 2011, Xaio, et al. 2001). After normalizing PECAM-1 expression to total vessel length, relative to sham- or 3VO-treated controls, we found that low-dose LPS induced expression of platelet endothelial

cell adhesion molecule-1 (PECAM-1) on the cortical vessel endothelium when combined with 3VO (5.39 ± 0.66; $p = 0.0020$ *vs.* 3VO/SAL, 3.19 ± 0.35; $p = 0.0006$ *vs.* Sham/LPS, 2.69 ± 0.68) (Figure 3C & D) (Hwang, et al. 2005). After normalizing IgG fluorescence intensity to total vessel length, we also found 3VO treatment induced deposition of serum IgG protein in the perivascular space (*3VO*/SAL, 0.67 ± 0.22; $p = 0.0003$ *vs.* Sham/LPS, 0.33 ± 0.14). Moreover, combined exposure to global ischemia and LPS enhanced this effect (3VO/LPS, 2.06 ± 0.75; $p = 0.0012$) consistent with progressive injury to the blood brain barrier (Figure 3C & E) (Cristante, et al. 2013).

3.3 Effects of ischemia and endotoxemia on peripheral neutrophil trafficking

Delayed neuronal death is a hallmark of GCI and reflects the cumulative effects of cell-autonomous apoptotic signaling, reactive neuroinflammation, and peripheral innate immune responses on the CNS. Given our observation that tissue injury in the 3VO/LPS paradigm peaked within the first 3 days, we next asked to what extent systemic priming influenced PMN recruitment to the post-ischemic brain (Chen, et al. 2014, Hirsch and Gordon 1983, Ullrich, et al. 2014). By Day 3, both 3VO/SAL (18.75 ± 10.04 PMN/mm^2; $p = 0.0374$ *vs.* Sham/SAL, 2.39 ± 0.81 PMN/mm^2) and 3VO/LPS treatment (48.60 ± 13.36 PMN/mm^2; $p < 0.0001$ *vs.* Sham/LPS, 2.93 ± 1.23 PMN/mm^2; $p = 0.0016$ *vs.* 3VO/SAL) induced cortical PMN margination above levels seen in controls (Figure 4A–B). The burden of PMN infiltration was directly proportional to the level of cortical injury observed (Pearson's $r = 0.82$, $p = 0.0002$) and inversely proportional to performance on tests of global neurological function (Pearson's $r = -0.89$, $p < 0.0001$) (Figure 4C).

Histological analyses indicated that systemic inflammation enhanced both cortical microglial activation and PMN recruitment in the post-ischemic cortex (Figure 5A–B) (Drago, et al. 2014). Global ischemia tripled levels of Iba1 staining in the cortex as compared to sham controls (32.24 ± 12.74; $p = 0.0085$ *vs.* Sham/SAL, 10.72 ± 5.69). Conversely, endotoxin challenge alone had little effect in this regard (Sham/LPS, 9.34 ± 4.01 *vs.* Sham/SAL; NS). When combined with global ischemia, LPS challenge had a marked effect on observed levels of microglial activation (71.20 ± 8.87; $p < 0.0001$ *vs.* Sham/LPS; $p = 0.0003$ *vs.* 3VO/SAL). Sholl analysis of microglial morphology confirmed the expected shift from the more ramified to an amoeboid appearance with ischemia, which was not observed with LPS challenge alone (Figure 5C). LPS-induced systemic inflammation enhanced the effect (Figure 5D) relative to ischemia alone ($p = 0.0187$). We also noted regional differences in the extent of microglial activation relative to the proportion of infiltrating PMNs (>60 cells/mm^2). Quantification of this effect by Sholl sub-analyses confirmed the correlation between increased PMN burden and microglial activation ($p = 0.0313$) that was dependent on systemic LPS administration (Figure 5E). However, the relationship between microglial activation and PMN burden was not observed in mice subjected to global ischemia alone ($p = 0.9338$). These findings suggest that in addition to inducing neuroinflammatory changes directly, systemic endotoxin induces a phenotypic shift in invading PMNs that influences the extent of microglial activation in the post-ischemic cortex.

3.4 Effects of cerebral ischemia and systemic endotoxemia on neutrophil priming

To directly assess the effect of low-dose LPS on peripheral immune activation, we next performed fluorescence cytometry on circulating, Ly-6G^{Hi}/CD11b^{Hi} PMNs (Figure 6). Ischemia alone was sufficient to activate PMNs in circulation at 2 hours post-reperfusion. While low-dose LPS resulted in a CD11b response that was comparable in magnitude, the effect persisted through the 6-hour time point likely due to the diffusion characteristics associated with IP delivery. Of note, combined 3VO/LPS challenge had synergistic effects on PMN CD11b expression (3VO/LPS MFI: 64,738) compared to ischemia alone (3VO/SAL MFI: 16,103).

3.5 Effects of cerebral ischemia and systemic endotoxemia on peripheral tissues

The accumulation of PMNs in somatic tissues is considered pathognomonic of acute reperfusion injury in a variety of disease models (Abraham 2003, Chaturvedi, et al. 2013, Marques, et al. 2012). And although the brain is hypersensitive to the effects of global ischemia, multi-organ failure is a common complication observed after successful return of spontaneous circulation (Partrick, et al. 1999, Partrick, et al. 1996). Given its close anatomical relationship with the cerebral circulation, we examined the extent to which cerebral ischemia and peripheral inflammation influenced PMN migration to the lung parenchyma. Within 3 days after GCI, we observed significant accumulations of PMNs in the lung (3VO/SAL, 2296.19 ± 532.50; $p = 0.019$ *vs.* Sham/SAL, 1417.72 ± 167.92). Low-dose LPS challenge following reperfusion doubled the observed effect (3VO/LPS, 3603.50 ± 374.64; $p = 0.0002$ *vs.* Sham/LPS, 1778.92 ± 315.28; $p = 0.0030$ *vs.* 3VO/SAL) (Figure 7A–B). We also assessed the extent of lung edema as a surrogate for lung injury. Relative to controls (Sham/SAL, 5.40 ± 1.10 μm; Sham/LPS, 5.03 ± 0.22 μm), exposure to either ischemia (3VO/SAL, 7.71 ± 0.74 μm; $p = 0.0312$ *vs.* Sham/SAL) or combined ischemia/endotoxin challenge (3VO/LPS, 10.80 ± 2.12 μm; $p = 0.0002$ *vs.* Sham/LPS; $p = 0.0189$ *vs.* 3VO/SAL) resulted in increased edema measured as alveolar wall thickness (Figure 7C). To extend this analysis further, we assessed the extent to which PMN migration was affected in other non-ischemic tissues. Data show that while neither GCI (liver, 76.19 ± 11.19; kidney, 19.30 ± 5.11) nor systemic LPS challenge (liver, 71.11 ± 21.37; kidney, 13.21 ± 2.03) influenced PMN migration above baseline, combined 3VO/LPS treatment was associated with increased PMN infiltration into both the non-ischemic liver (226.19 ± 122.87; $p = 0.0199$ *vs.* 3VO/SAL, $p = 0.0199$ *vs.* Sham/LPS) and kidney (32.51 ± 2.35; $p = 0.0159$ *vs.* 3VO/SAL, $p = 0.0015$ *vs.* Sham/LPS). We also performed H&E staining on tissue sections and found that PMN infiltration was not otherwise associated with injury to the liver or kidney (Figure S4).

4. DISCUSSION

In the present study, we tested the hypothesis that occult endotoxemia has important effects on the CNS when associated with global ischemia. Our results revealed three main findings. First, we found that low-dose LPS challenge enhances post-ischemic damage in the CNS with secondary effects on microvascular inflammation, injury to the BBB, and a shift in both microglial and PMN activation. Second, we found that combined 3VO/LPS challenge exerted distinct effects on the activation and homing of PMNs within and outside the CNS.

Third, our data suggests the testable hypothesis that immunological coupling between the lung and brain alters cumulative injury after cardiac arrest and likely other diseases in which cerebral ischemia is a central component.

The pathological events contributing to ischemic brain injury are both temporally and mechanistically diverse (Dirnagl, et al. 2007). Within minutes, nutrient deprivation and secondary glutamate-dependent excitotoxicity induce necrosis and apoptosis, among other molecularly distinct forms of injury, in vulnerable CNS populations (Heiss 2012). While models of global ischemia are often used to study the molecular basis of CA1 hippocampal degeneration, selective neuronal vulnerability and loss are recognized in other brain regions (Ito, et al. 2013, Pulsinelli and Brierley 1979, Thal, et al. 2010, Yonekura, et al. 2004) and are observed in our model (Figure S3). At the bedside, changes on the clinical exam, brain imaging, and increased levels of neuron-specific enolase all reflect the evolution of such pathological cascades (Calderon, et al. 2014). The role of systemic inflammation in post-ischemic neurodegeneration is also well recognized (Samborska-Sablik, et al. 2011, Vaahersalo, et al. 2014). For example, serum levels of IL-6 and other cytokines correlate with poor neurologic recovery after cardiac arrest and in-hospital death following ischemic stroke (Rallidis, et al. 2006, Vaahersalo, et al. 2014). And in the case of prolonged cardiac arrest, the induced cytokine storm produces endothelial dysfunction, coagulation defects, and multi-organ failure mimicking septic shock (Adrie, et al. 2002). Given the global nature of the injury and the dynamic interplay between cell-autonomous and post-ischemic inflammation, it is not surprising that the odds of surviving an out of hospital cardiac arrest is less than one in five. Given the skepticism regarding the benefit of targeted temperature management, there remains an urgent need to find alternate therapies targeting these and other precipitating pathologies (Bro-Jeppesen, et al. 2014).

As an alternative to existing models of cardiac arrest (Kofler, et al. 2004, Liachenko, et al. 1998), we used the mouse 3-vessel occlusion model because of its reproducibility and the ability to control the timing and severity of ischemia. The use of low-dose endotoxin as a driver of PCAS pathology is a unique feature of this work and is based on reports from the clinical literature citing the association between serum endotoxin and the duration of post cardiac arrest shock (Grimaldi, et al. 2013, Grimaldi, et al. 2015). Mesenteric ischemia stimulates the growth of gram-negative bacteria *in situ* and induces villous blunting with mucosal degeneration (Karhausen, et al. 2013, L'Her, et al. 2005, Wang, et al. 2012). In our initial dose ranging studies, we found the delivery of LPS above 1 mg/kg after the 3VO procedure caused a high rate of perioperative mortality (data not shown). We, therefore, adjusted our dosing strategy reducing the amount of LPS (50 μg/kg) to a point where serum endotoxin was undetectable, such as has been described for a significant number of patients (Grimaldi, et al. 2015). Although low-dose endotoxin challenge was not detected in serum using the limulus amebocyte lysate assay, which is sensitive to levels as low as 0.1 EU/ml (or approximately 0.01 ng endotoxin/ml), its use in our paradigm resulted in the activation of brain endothelium, damage to the BBB with the accumulation of serum proteins in the parenchyma, microglial activation, and the accumulation of PMNs in areas of cortical ischemia. Thus, while the 3VO procedure remains a surrogate for cardiac arrest, many of the pathological changes described in the post-cardiac arrest syndrome were recapitulated in our model (Blomqvist and Wieloch 1985, Hossmann and Hossmann 1973).

The pulmonary endothelium plays an active role in regulating the priming of PMNs during their transit through the systemic circulation (Aoyama-Ishikawa, et al. 2014, Singh, et al. 2012). In the mouse model of sepsis, the pro-inflammatory milieu caused by endotoxin challenge impairs lung-mediated PMN de-priming, resulting in their accumulation, priming, release to the systemic circulation. Cerebral ischemia and systemic endotoxin had distinct effects on PMN activation. While ischemia-induced transient PMN CD11b expression (<2 hours), the relative fraction of Ly-6G(+) PMNs compared with other leukocytes increased over time, suggesting an initial sequestration of primed PMNs and subsequent de-priming and release, observed previously following low-dose LPS treatment (Copeland, et al. 2005). However, in our hands, low-dose endotoxin challenge induced the sustained priming of circulating PMNs, which when combined with ischemia, induced CD11b levels above the sum of the individual stimuli lasting up to 6 hours post-treatment. In our case, systemic LPS induced the infiltration of PMNs to the lung and pulmonary interstitial edema. These data suggest that combined ischemia with endotoxin challenge induced lung injury, overwhelming endogenous de-priming mechanisms, and allowed activated PMNs to persist in the systemic circulation. Notably, PMN CD11b expression levels returned to baseline levels in all treatment groups within 3 days reflecting the recovery or induction of endogenous anti-inflammatory mechanisms.

Modern post-resuscitation management of patients surviving out-of-hospital cardiac arrest (OHCA) includes the use of targeted temperature management, percutaneous coronary intervention, and supportive measures with the goal of improving the odds of survival with good neurologic recovery (Kocjancic, et al. 2014). There has been a recent interest in investigating the benefit of prophylactic antibiotics as a means to limit pathogen-associated systemic inflammatory responses particularly in patients with evidence of aspiration or those treated with systemic hypothermia (Hellenkamp, et al. 2016, Ribaric, et al. 2017). For example, Davies et al. reported in a series of 138 patients that the early use of antibiotics was associated with a mortality benefit (Davies, et al. 2013). Other reports have been less optimistic, reducing the incidence of pneumonia without influencing all-cause mortality (Gagnon, et al. 2015, Tagami, et al. 2016). While our model induced systemic inflammation using LPS, there is sufficient evidence that damage to the enteric system results in the release of coliform species into the systemic circulation. Thus, the optimal antibiotic therapy in OHCA would cover both respiratory and enteric organisms, suppress bacterial growth (bacteriostatic), and would exhibit limited bactericidal activity limiting membrane breakdown and LPS release that would compound PAMP-mediated systemic inflammation and reperfusion injury. Of note, in addition to their bacteriostatic effects on gram-positive and gram-negative organisms, the non-antibiotic properties of the tetracycline class of antibiotics have garnered interest given their anti-inflammatory properties and protective effects toward lung injury in models of ischemia-reperfusion with sepsis (Roy, et al. 2012).

Although under-appreciated, the extent of pulmonary involvement following cerebral ischemia, and combined ischemia/endotoxin challenge, in particular, has important clinical implications. Pulmonary complications including pneumonia, neurogenic pulmonary edema, and acute respiratory distress syndrome are frequently seen in patients presenting with acute stroke, traumatic brain injury, and other acute neurological injuries (Balofsky, et al. 2017). Contributing factors include an underlying increased risk for aspiration and the pro-

inflammatory effects of damage- and pathogen-associated molecular patterns released from the brain and portal system. Through a first-pass effect involving the lung, these factors produce endothelial dysfunction and capillary permeability with possible priming effects on circulating PMNs as they travel en passant through the lung microvasculature. Similar to the model initially proposed by Mascia et al. (Mascia 2009), our data indicate that low-dose endotoxin provides the 'second hit' promoting PMN activation, infiltration into the lung parenchyma, and secondary injury. In conditions where local inflammation goes unchecked, the lung can confer secondary organ damage in a feed-forward mechanism. This concept is supported by the increased level of brain injury and trafficking of PMNs to the non-ischemic liver and kidney seen in our model. Based on these observations, it is reasonable to assume that pre-existing lung disease, barotrauma, or hyperoxic exposure introduced following endotracheal intubation likely influence delayed neurodegeneration through effects on the lung and its ability to regulate PMN priming and other systemic immune responses.

In summary, we investigated the impact of low-dose LPS challenge in a mouse model of GCI to understand better the impact of systemic inflammation on delayed post-ischemic neurodegeneration. Our results demonstrate that when combined with GCI, serologically occult endotoxin can reproduce the neurovascular injury, neuroinflammation, and damage to peripheral targets including the lung, liver, and kidney commonly seen following cardiac arrest. Furthermore, these findings suggest that the lung serves as a gatekeeper of systemic immune responses in cerebrovascular disorders and that underlying factors such as pre-existing lung disease may have a direct bearing on the extent of multisystem organ dysfunction observed. As a corollary to these findings, we predict that targeted manipulation of the local inflammatory milieu of the lung could provide neuroprotective benefit to patients following cardiac arrest.

Supplementary Material

Refer to Web version on PubMed Central for supplementary material.

Acknowledgments

The authors would like to thank Minsoo Kim, Yelena Lerman, and Alison Gaylo for their assistance in conducting flow cytometric measurements of neutrophil activation, Rupal Mehta and Orestes Solis for hematoxylin and eosin staining of peripheral organs, Craig Morrell for assistance with granulocyte counts, and Kevin Mazurek for assistance with MATLAB.

SOURCES OF FUNDING

These studies were supported by the Schmitt Program on Integrative Brain Research and awards from the National Institutes of Health to MWH (R01-NS092455) and the Institutional MSTP training grant (NIH/T32-GM007356) and fellowship funding to NM (F30-NS092168) from the NIH.

ABBREVIATIONS

3vo	three-vessel occlusion
ANOVA	analysis of variance
AU	arbitrary units

BAO	basilar artery occlusion
BBB	blood-brain barrier
BCCAO	bilateral common carotid artery occlusion
CBF	cerebral blood flow
CCA	common carotid artery
CNS	central nervous system
DAMP	damage-associated molecular pattern
EU	endotoxin unit
FSC	forward scatter
GCI	global cerebral ischemia
IHC	immunohistochemistry
IP	intraperitoneal
LPS	lipopolysaccharide
MAP2	microtubule-associated protein 2
OHCA	out-of-hospital cardiac arrest
PAMP	pathogen-associated molecular pattern
PCAS	post-cardiac arrest syndrome
PECAM-1	platelet and endothelial cell adhesion molecule 1
PMN	polymorphonuclear neutrophil
SAL	saline
SSC	side scatter

References

Abella BS, Zhao D, Alvarado J, Hamann K, Vanden Hoek TL, Becker LB. Intra-arrest cooling improves outcomes in a murine cardiac arrest model. Circulation. 2004; 109:2786–2791. [PubMed: 15159295]

Abraham E. Neutrophils and acute lung injury. Critical care medicine. 2003; 31:S195–199. [PubMed: 12682440]

Adrie C, Adib-Conquy M, Laurent I, Monchi M, Vinsonneau C, Fitting C, et al. Successful cardiopulmonary resuscitation after cardiac arrest as a “sepsis-like” syndrome. Circulation. 2002; 106:562–568. [PubMed: 12147537]

Adrie C, Laurent I, Monchi M, Cariou A, Dhainaou JF, Spaulding C. Postresuscitation disease after cardiac arrest: A sepsis-like syndrome? Current opinion in critical care. 2004; 10:208–212. [PubMed: 15166838]

Annane D, Sharshar T. Cognitive decline after sepsis. Lancet Respir Med. 2015; 3:61–69. [PubMed: 25434614]

Aoyama-Ishikawa M, Seishu A, Kawakami S, Maeshige N, Miyoshi M, Ueda T, et al. Intravenous immunoglobulin-induced neutrophil apoptosis in the lung during murine endotoxemia. Surgical infections. 2014; 15:36–42. [PubMed: 24116740]

Balofsky A, George J, Papadakos P. Neuropulmonology. Handb Clin Neurol. 2017; 140:33–48. [PubMed: 28187807]

Becker KJ, Kalil AJ, Tanzi P, Zierath DK, Savos AV, Gee JM, et al. Autoimmune responses to the brain after stroke are associated with worse outcome. Stroke; a journal of cerebral circulation. 2011; 42:2763–2769.

Bernard SA, Gray TW, Buist MD, Jones BM, Silvester W, Gutteridge G, et al. Treatment of comatose survivors of out-of-hospital cardiac arrest with induced hypothermia. The New England journal of medicine. 2002; 346:557–563. [PubMed: 11856794]

Blomqvist P, Wieloch T. Ischemic brain damage in rats following cardiac arrest using a long-term recovery model. Journal of cerebral blood flow and metabolism: official journal of the International Society of Cerebral Blood Flow and Metabolism. 1985; 5:420–431.

Bro-Jeppesen J, Kjaergaard J, Wanscher M, Nielsen N, Friberg H, Bjerre M, et al. The inflammatory response after out-of-hospital cardiac arrest is not modified by targeted temperature management at 33 degrees c or 36 degrees c. Resuscitation. 2014; 85:1480–1487. [PubMed: 25150183]

Calderon LM, Guyette FX, Doshi AA, Callaway CW, Rittenberger JC. Post Cardiac Arrest S. Combining nse and s100b with clinical examination findings to predict survival after resuscitation from cardiac arrest. Resuscitation. 2014; 85:1025–1029. [PubMed: 24795283]

Cardiff RD, Miller CH, Munn RJ. Manual hematoxylin and eosin staining of mouse tissue sections. Cold Spring Harb Protoc. 2014; 2014:655–658. [PubMed: 24890205]

Casey LC, Balk RA, Bone RC. Plasma cytokine and endotoxin levels correlate with survival in patients with the sepsis syndrome. Ann Intern Med. 1993; 119:771–778. [PubMed: 8379598]

Chamak B, Fellous A, Glowinski J, Prochiantz A. Map2 expression and neuritic outgrowth and branching are coregulated through region-specific neuro-astroglial interactions. The Journal of neuroscience: the official journal of the Society for Neuroscience. 1987; 7:3163–3170. [PubMed: 2444676]

Chaturvedi S, Yuen DA, Bajwa A, Huang YW, Sokollik C, Huang L, et al. Slit2 prevents neutrophil recruitment and renal ischemia-reperfusion injury. Journal of the American Society of Nephrology: JASN. 2013; 24:1274–1287. [PubMed: 23766538]

Chen L, Marko L, Kassmann M, Zhu Y, Wu K, Gollasch M. Role of trpv1 channels in ischemia/reperfusion-induced acute kidney injury. PloS one. 2014; 9:e109842. [PubMed: 25330307]

Copeland S, Warren HS, Lowry SF, Calvano SE, Remick D, et al. Inflammation. Acute inflammatory response to endotoxin in mice and humans. Clinical and diagnostic laboratory immunology. 2005; 12:60–67. [PubMed: 15642986]

Coultrap SJ, Vest RS, Ashpole NM, Hudmon A, Bayer KU. Camkii in cerebral ischemia. Acta pharmacologica Sinica. 2011; 32:861–872. [PubMed: 21685929]

Cristante E, McArthur S, Mauro C, Maggioli E, Romero IA, Wylezinska-Arridge M, et al. Identification of an essential endogenous regulator of blood-brain barrier integrity, and its pathological and therapeutic implications. Proceedings of the National Academy of Sciences of the United States of America. 2013; 110:832–841. [PubMed: 23277546]

Davies KJ, Walters JH, Kerslake IM, Greenwood R, Thomas MJ. Early antibiotics improve survival following out-of hospital cardiac arrest. Resuscitation. 2013; 84:616–619. [PubMed: 23153650]

Deierborg T, Wieloch T, Diano S, Warden CH, Horvath TL, Mattiasson G. Overexpression of ucp2 protects thalamic neurons following global ischemia in the mouse. Journal of cerebral blood flow and metabolism: official journal of the International Society of Cerebral Blood Flow and Metabolism. 2008; 28:1186–1195.

Denes A, Ferenczi S, Kovacs KJ. Systemic inflammatory challenges compromise survival after experimental stroke via augmenting brain inflammation, blood- brain barrier damage and brain oedema independently of infarct size. Journal of neuroinflammation. 2011; 8:164. [PubMed: 22114895]

Dirnagl U, Klehmet J, Braun JS, Harms H, Meisel C, Ziemssen T, et al. Stroke-induced immunodepression: Experimental evidence and clinical relevance. Stroke; a journal of cerebral circulation. 2007; 38:770–773.

Drago F, Sautiere PE, Le Marrec-Croq F, Accorsi A, Van Camp C, Salzet M, et al. Microglia of medicinal leech (hirudo medicinalis) express a specific activation marker homologous to vertebrate ionized calcium-binding adapter molecule 1 (iba1/alias aif-1). Developmental neurobiology. 2014; 74:987–1001. [PubMed: 24723370]

Ferreira TA, Blackman AV, Oyrer J, Jayabal S, Chung AJ, Watt AJ, et al. Neuronal morphometry directly from bitmap images. Nature methods. 2014; 11:982–984. [PubMed: 25264773]

Gagnon DJ, Nielsen N, Fraser GL, Riker RR, Dziodzio J, Sunde K, et al. Prophylactic antibiotics are associated with a lower incidence of pneumonia in cardiac arrest survivors treated with targeted temperature management. Resuscitation. 2015; 92:154–159. [PubMed: 25680823]

Grimaldi D, Guivarch E, Neveux N, Fichet J, Pene F, Marx JS, et al. Markers of intestinal injury are associated with endotoxemia in successfully resuscitated patients. Resuscitation. 2013; 84:60–65. [PubMed: 22743354]

Grimaldi D, Sauneuf B, Guivarch E, Ricome S, Geri G, Charpentier J, et al. High level of endotoxemia following out-of-hospital cardiac arrest is associated with severity and duration of postcardiac arrest shock. Crit Care Med. 2015; 43:2597–2604. [PubMed: 26427593]

Heiss WD. The ischemic penumbra: How does tissue injury evolve? Annals of the New York Academy of Sciences. 2012; 1268:26–34. [PubMed: 22994218]

Hellenkamp K, Onimischewski S, Kruppa J, Fasshauer M, Becker A, Eiffert H, et al. Early pneumonia and timing of antibiotic therapy in patients after nontraumatic out-of-hospital cardiac arrest. Critical care. 2016; 20:31. [PubMed: 26831508]

Highland MA, Schneider DA, White SN, Madsen-Bouterse SA, Knowles DP, Davis WC. Differences in leukocyte differentiation molecule abundances on domestic sheep (ovis aries) and bighorn sheep (ovis canadensis) neutrophils identified by flow cytometry. Comp Immunol Microbiol Infect Dis. 2016; 46:40–46. [PubMed: 27260809]

Hirsch S, Gordon S. Polymorphic expression of a neutrophil differentiation antigen revealed by monoclonal antibody 7/4. Immunogenetics. 1983; 18:229–239. [PubMed: 6618532]

Hoesch RE, Koenig MA, Geocadin RG. Coma after global ischemic brain injury: Pathophysiology and emerging therapies. Critical care clinics. 2008; 24:25–44. vii–viii. [PubMed: 18241777]

Hossmann V, Hossmann KA. Return of neuronal functions after prolonged cardiac arrest. Brain research. 1973; 60:423–438. [PubMed: 4763617]

Hwang IK, Kim DW, Yoo KY, Jung BK, Song JH, Jung JY, et al. Ischemia-induced changes of platelet endothelial cell adhesion molecule-1 in the hippocampal ca1 region in gerbils. Brain research. 2005; 1048:251–257. [PubMed: 15913570]

Ito U, Hakamata Y, Yamaguchi T, Ohno K. Cerebral ischemia model using mongolian gerbils-comparison between unilateral and bilateral carotid occlusion models. Acta neurochirurgica. Supplement. 2013; 118:17–21. [PubMed: 23564098]

Karhausen J, Qing M, Gibson A, Moeser AJ, Griefingholt H, Hale LP, et al. Intestinal mast cells mediate gut injury and systemic inflammation in a rat model of deep hypothermic circulatory arrest. Critical care medicine. 2013; 41:e200–210. [PubMed: 23478660]

Kliper E, Bashat DB, Bornstein NM, Shenhar-Tsarfaty S, Hallevi H, Auriel E, et al. Cognitive decline after stroke: Relation to inflammatory biomarkers and hippocampal volume. Stroke; a journal of cerebral circulation. 2013; 44:1433–1435.

Kocjancic ST, Jazbec A, Noc M. Impact of intensified postresuscitation treatment on outcome of comatose survivors of out-of-hospital cardiac arrest according to initial rhythm. Resuscitation. 2014; 85:1364–1369. [PubMed: 25010782]

Kofler J, Hattori K, Sawada M, DeVries AC, Martin LJ, Hurn PD, et al. Histopathological and behavioral characterization of a novel model of cardiac arrest and cardiopulmonary resuscitation in mice. Journal of neuroscience methods. 2004; 136:33–44. [PubMed: 15126043]

L'Her E, Cassaz C, Le Gal G, Cholet F, Renault A, Boles JM. Gut dysfunction and endoscopic lesions after out-of-hospital cardiac arrest. Resuscitation. 2005; 66:331–334. [PubMed: 16039032]

Liachenko S, Tang P, Hamilton RL, Xu Y. A reproducible model of circulatory arrest and remote resuscitation in rats for nmr investigation. Stroke; a journal of cerebral circulation. 1998; 29:1229–1238. discussion 1238–1229.

Marques PE, Amaral SS, Pires DA, Nogueira LL, Soriani FM, Lima BH, et al. Chemokines and mitochondrial products activate neutrophils to amplify organ injury during mouse acute liver failure. Hepatology. 2012; 56:1971–1982. [PubMed: 22532075]

Mascia L. Acute lung injury in patients with severe brain injury: A double hit model. Neurocrit Care. 2009; 11:417–426. [PubMed: 19548120]

Neumar RW, Nolan JP, Adrie C, Aibiki M, Berg RA, Bottiger BW, et al. Post-cardiac arrest syndrome: Epidemiology, pathophysiology, treatment, and prognostication. Circulation. 2008; 118:2452–2483. [PubMed: 18948368]

Paradis, NA. Cardiac arrest: The science and practice of resuscitation medicine. Cambridge, UK: New York: Cambridge University Press; 2007.

Partrick DA, Moore EE, Fullerton DA, Barnett CC Jr, Meldrum DR, Silliman CC. Cardiopulmonary bypass renders patients at risk for multiple organ failure via early neutrophil priming and late neutrophil disability. The Journal of surgical research. 1999; 86:42–49. [PubMed: 10452867]

Partrick DA, Moore FA, Moore EE, Barnett CC Jr, Silliman CC. Neutrophil priming and activation in the pathogenesis of postinjury multiple organ failure. New horizons. 1996; 4:194–210. [PubMed: 8774796]

Peres Bota D, Lopes Ferreira F, Melot C, Vincent JL. Body temperature alterations in the critically ill. Intensive care medicine. 2004; 30:811–816. [PubMed: 15127194]

Pittman K, Kubes P. Damage-associated molecular patterns control neutrophil recruitment. J Innate Immun. 2013; 5:315–323. [PubMed: 23486162]

Popp A, Jaenisch N, Witte OW, Frahm C. Identification of ischemic regions in a rat model of stroke. PloS one. 2009; 4:e4764. [PubMed: 19274095]

Pulsinelli WA, Brierley JB. A new model of bilateral hemispheric ischemia in the unanesthetized rat. Stroke; a journal of cerebral circulation. 1979; 10:267–272.

Rallidis LS, Vikelis M, Panagiotakos DB, Rizos I, Zolindaki MG, Kaliva K, et al. Inflammatory markers and in-hospital mortality in acute ischaemic stroke. Atherosclerosis. 2006; 189:193–197. [PubMed: 16388807]

Ribaric SF, Turel M, Knafelj R, Gorjup V, Stanic R, Gradisek P, et al. Prophylactic versus clinically-driven antibiotics in comatose survivors of out-of-hospital cardiac arrest-a randomized pilot study. Resuscitation. 2017; 111:103–109. [PubMed: 27987397]

Ridder DA, Schwaninger M. Nf-kappab signaling in cerebral ischemia. Neuroscience. 2009; 158:995–1006. [PubMed: 18675321]

Rodriguez JA, Sobrino T, Orbe J, Purroy A, Martinez-Vila E, Castillo J, et al. Prometalloproteinase-10 is associated with brain damage and clinical outcome in acute ischemic stroke. Journal of thrombosis and haemostasis: JTH. 2013; 11:1464–1473. [PubMed: 23742289]

Roy SK, Kubiak BD, Albert SP, Vieau CJ, Gatto L, Golub L, et al. Chemically modified tetracycline 3 prevents acute respiratory distress syndrome in a porcine model of sepsis + ischemia/reperfusion-induced lung injury. Shock. 2012; 37:424–432. [PubMed: 22258231]

Samborska-Sablik A, Sablik Z, Gaszynski W. The role of the immuno-inflammatory response in patients after cardiac arrest. Archives of medical science: AMS. 2011; 7:619–626. [PubMed: 22291797]

Schmued LC, Stowers CC, Scallet AC, Xu L. Fluoro-jade c results in ultra high resolution and contrast labeling of degenerating neurons. Brain research. 2005; 1035:24–31. [PubMed: 15713273]

Singh NR, Johnson A, Peters AM, Babar J, Chilvers ER, Summers C. Acute lung injury results from failure of neutrophil de-priming: A new hypothesis. European journal of clinical investigation. 2012; 42:1342–1349. [PubMed: 22984929]

Tadie JM, Bae HB, Jiang S, Park DW, Bell CP, Yang H, et al. Hmgb1 promotes neutrophil extracellular trap formation through interactions with toll-like receptor 4. American journal of physiology. Lung cellular and molecular physiology. 2013; 304:L342–349. [PubMed: 23316068]

Tagami T, Matsui H, Kuno M, Moroe Y, Kaneko J, Unemoto K, et al. Early antibiotics administration during targeted temperature management after out-of-hospital cardiac arrest: A nationwide database study. BMC Anesthesiol. 2016; 16:89. [PubMed: 27717334]

Thal SC, Thal SE, Plesnila N. Characterization of a 3-vessel occlusion model for the induction of complete global cerebral ischemia in mice. Journal of neuroscience methods. 2010; 192:219–227. [PubMed: 20688105]

Ullrich N, Strecker JK, Minnerup J, Schilling M. The temporo-spatial localization of polymorphonuclear cells related to the neurovascular unit after transient focal cerebral ischemia. Brain research. 2014; 1586:184–192. [PubMed: 25152468]

Vaahersalo J, Skrifvars MB, Pulkki K, Stridsberg M, Rosjo H, Hovilehto S, et al. Admission interleukin-6 is associated with post resuscitation organ dysfunction and predicts long-term neurological outcome after out-of-hospital ventricular fibrillation. Resuscitation. 2014; 85:1573–1579. [PubMed: 25238742]

Wang C, Wang H, Chang DY, Hao J, Zhao MH, Chen M. High mobility group box 1 contributes to anti-neutrophil cytoplasmic antibody-induced neutrophils activation through receptor for advanced glycation end products (rage) and toll-like receptor 4. Arthritis Res Ther. 2015; 17:64. [PubMed: 25889374]

Wang F, Li Q, Wang C, Tang C, Li J. Dynamic alteration of the colonic microbiota in intestinal ischemia-reperfusion injury. PloS one. 2012; 7:e42027. [PubMed: 22848694]

Xaio H, Banks WA, Niehoff ML, Morley JE. Effect of lps on the permeability of the blood-brain barrier to insulin. Brain research. 2001; 896:36–42. [PubMed: 11277970]

Yao X, Derugin N, Manley GT, Verkman AS. Reduced brain edema and infarct volume in aquaporin-4 deficient mice after transient focal cerebral ischemia. Neurosci Lett. 2015; 584:368–372. [PubMed: 25449874]

Yonekura I, Kawahara N, Nakatomi H, Furuya K, Kirino T. A model of global cerebral ischemia in c57 bl/6 mice. Journal of cerebral blood flow and metabolism: official journal of the International Society of Cerebral Blood Flow and Metabolism. 2004; 24:151–158.

HIGHLIGHTS

- Transient endotoxemia exacerbates CNS injury when combined with global ischemia.
- Global ischemia and LPS exhibit synergistic effects on PMN activation.
- Combined 3VO/LPS induces PMN homing to the brain, lung, and non-ischemic organs.
- Lung-brain coupling modulates post-ischemic injury and innate immune responses.

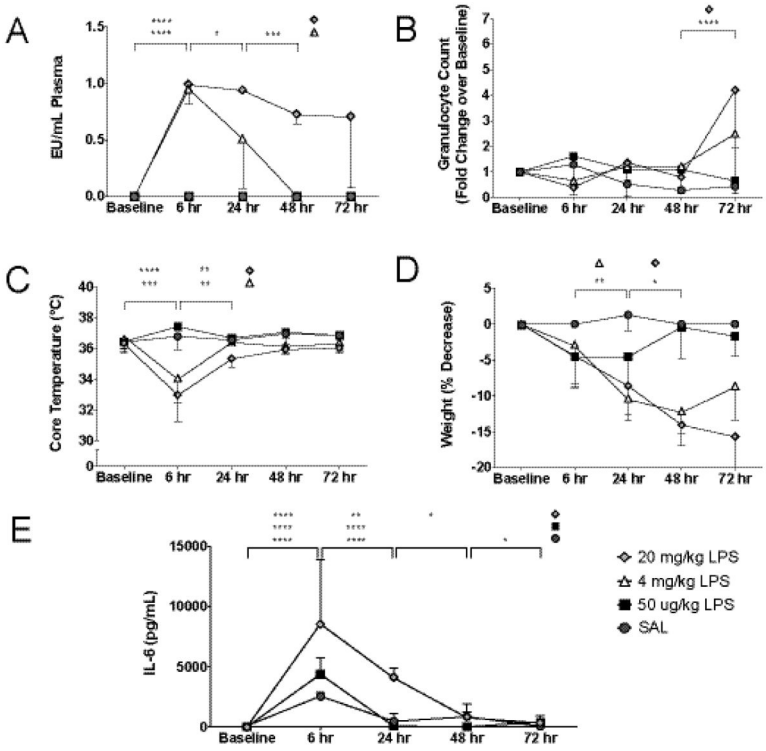

Figure 1.

LPS dose titration studies. IP administration of 50 μg/kg LPS yielded undetectable plasma endotoxin (A) and no changes in granulocyte count (B), core temperature (C), or weight (D), while effects were seen with 4 mg/kg and 20 mg/kg. (D) Elevated IL-6 was seen in all mice after 6 hours and remained elevated at 24 hours in mice receiving 20 mg/kg LPS. Values represent means ± SD (n = 3). 1-way ANOVA: * $p < 0.05$, ** $p < 0.01$, *** $p < 0.001$, **** $p < 0.0001$.

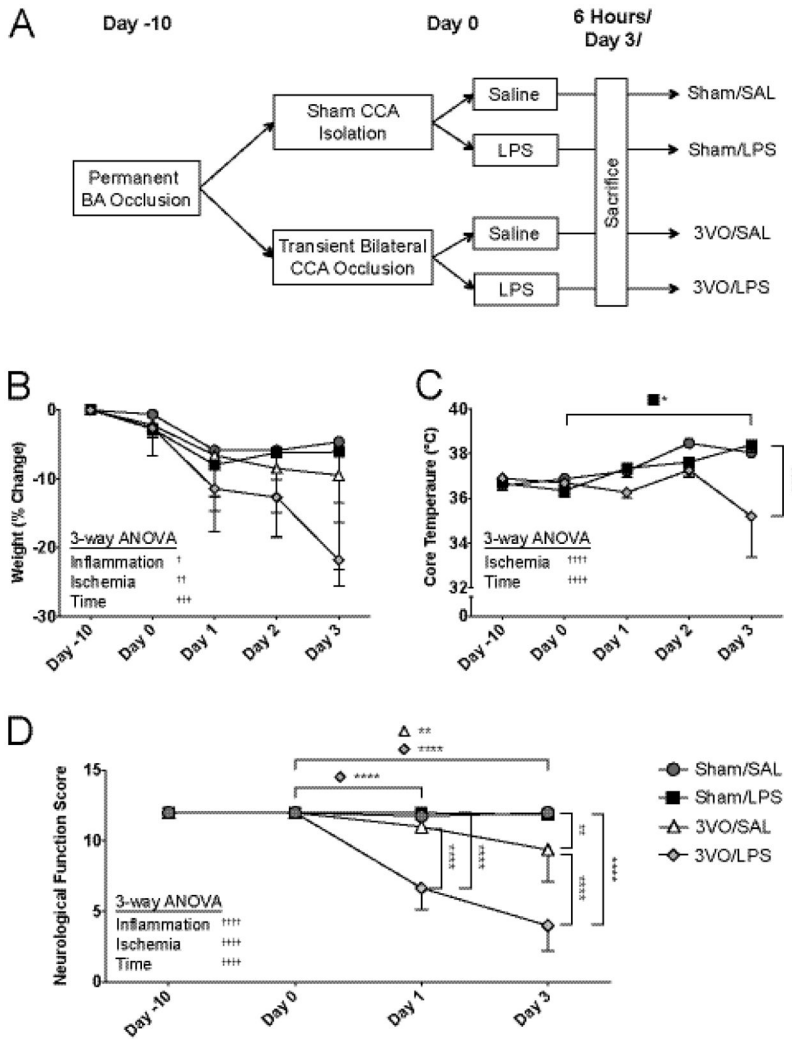

Figure 2.

Analyses of combined 3VO and systemic LPS on neurological function. (A) Following basilar artery (BA) occlusion, mice undergo either sham dissection or 15-minute common carotid artery (CCA) occlusion with saline or IP LPS injection immediately following reperfusion. Effects of experimental procedures on weight (B) and core temperature (C). (D) Effects of experimental procedures on neurological functional scores assessed prior to BAO (Day −10), prior to BCCAO/sham (Day 0), at Day 1, and at Day 3. Values represent means ± SD (n = 3–4 per group). 3-way ANOVA: † ANOVA main effects, * Dunn-Sidak multiple comparisons. */† $p < 0.05$, **/†† $p < 0.01$, ††† $p < 0.001$, ****/†††† $p < 0.0001$.

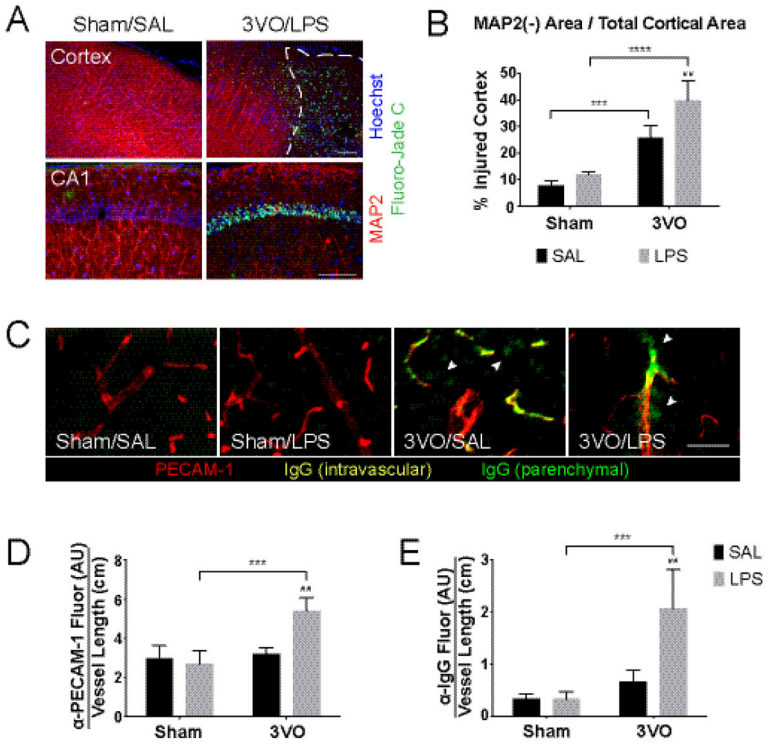

Figure 3.

Effects of systemic LPS exposure on ischemia-induced cortical injury. (A) IHC of coronal brain sections demonstrates combined effects of 3VO/LPS treatment on dendritic injury (beading, loss of MAP2 staining; red) and neuron death (Fluoro-Jade C; green) on cortex (top) and CA1 of the hippocampus (bottom); scale bars = 100 μm. White dashed line outlines area of MAP2(−) cortex. (B) Histogram illustrating exacerbated injury caused by the addition of LPS after 3VO. % Injured cortex = MAP2(−) area, as outlined in (A, top), over total cortical area. (C) Combined 3VO and endotoxemia causes PECAM-1 upregulation (red) and parenchymal IgG deposition (green; white arrowheads); scale bar = 100 μm. 3VO/LPS treatment upregulates vascular PECAM-1 expression (D) and IgG deposition per vessel length (E) in 3VO/LPS animals. Values represent means ± SD (n = 3–4 per group). AU = arbitrary units. 2-way ANOVA: * Sham *vs.* 3VO; $^{\#}$ SAL *vs.* LPS. $^{\#\#}$ $p < 0.01$, *** $p < 0.001$, **** $p < 0.0001$.

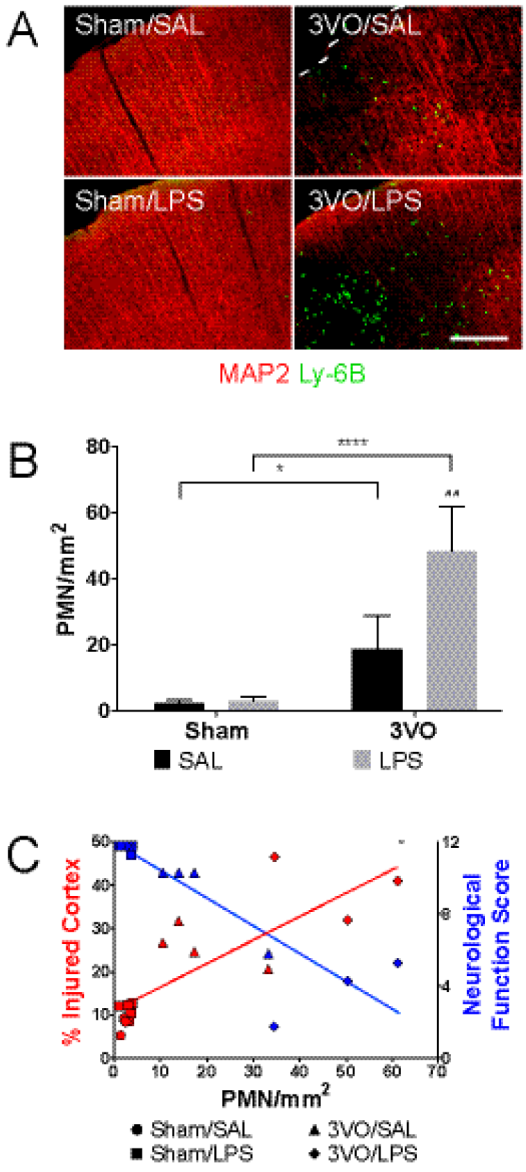

Figure 4.

IP LPS treatment enhances PMN accumulation in post-ischemic cortex at Day 3. IHC of cortical sections (A) and histogram (B) demonstrating Ly-6B(+) PMN infiltration after ischemia-reperfusion; scale bar = 200 μm. 2-way ANOVA: * Sham *vs.* 3VO; $^{\#}$ SAL *vs.* LPS. * $p < 0.05$, $^{\#\#}$ $p < 0.01$, **** $p < 0.0001$. (C) Correlation between PMN infiltration and cortical injury; Pearson's $r = 0.8177$, $p = 0.0002$. Inverse relationship between PMN infiltration and Neurological Function Score; Pearson's $r = -0.8877$, $p < 0.0001$. Values represent means ± SD (n = 3–4 per group).

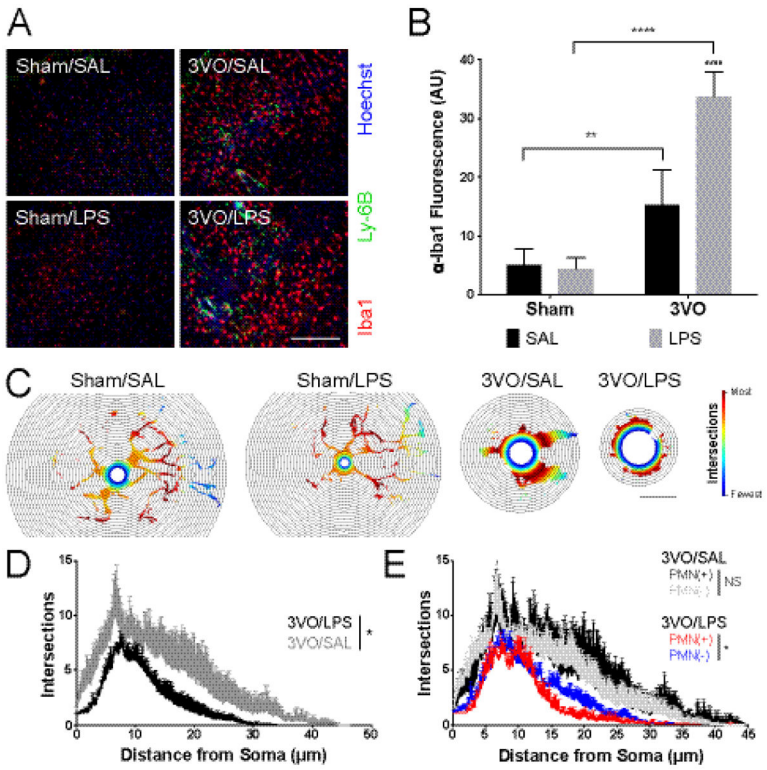

Figure 5.

Delayed effects of systemic LPS and PMN migration on neuroinflammation. (A) Immunohistochemical analyses of microglial activation (Iba1; red) and cortical PMN (Ly-6B; green) migration 3 days following treatment; scale bar = 100 μm. (B) Stimulatory effect of systemic LPS treatment on microglial activation after GCI assessed using average Iba1 fluorescence intensity per mm^2 field. 2-way ANOVA: * Sham *vs.* 3VO; $^{\#}$ SAL *vs.* LPS. ** $p < 0.01$, ****/#### $p < 0.0001$. (C) Representative heat maps illustrating differences in microglial arborization across treatment groups. Heat maps are cell-specific with red indicating the radius with the greatest number intersections; scale bar = 15 μm. (D) Sholl analysis of microglia in 3VO/SAL vs. 3VO/LPS animals. (E) Sholl analysis demonstrating blunted arborization in microglia in PMN-rich cortex of 3VO/LPS mice. Values represent means ± SD (n = 3–4 per group). Repeated measures ANOVA: * $p < 0.05$, NS = no significant difference between PMN(+) and PMN(−) cortex. Values represent means ± SD (n = 3–4 per group).

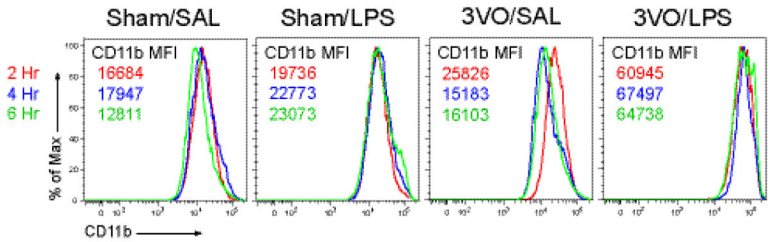

Figure 6.

Timing of peripheral neutrophil priming in the GCI model. Flow cytometry analyses demonstrating the effects of systemic inflammation (Sham/LPS), GCI (3VO/SAL), and combined treatment (3VO/LPS) on CD11b expression on peripheral Ly-6G^{Hi}/CD11b^{Hi} PMNs 2, 4, and 6 hours after reperfusion compared to Sham/SAL-treated mice. Values represent 10,000 events per time point per group.

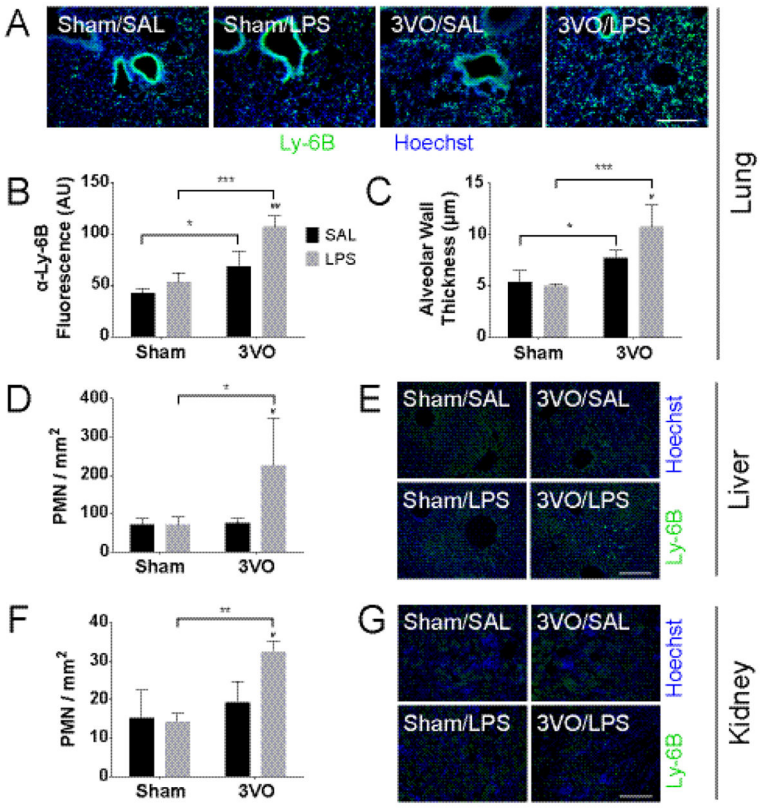

Figure 7.

LPS enhances PMN accumulation in peripheral organs after GCI. Lung IHC (A) and quantitative analyses for average fluorescence intensity of Ly-6B(+) PMNs per mm^2 field (B) and alveolar wall thickness (C). PMN accumulation is observed in the liver (D–E) and kidney (F–G) with 3VO/LPS treatment but not with 3VO/SAL. Scale bars = 200 μm. Values represent means ± SD (n = 3–4 per group). AU = arbitrary units. 2-way ANOVA: * Sham *vs.* 3VO; # SAL *vs.* LPS. */# $p < 0.05$, **/## $p < 0.01$, *** $p < 0.001$.